Distributed Strapdown Inertial Navigation System Error and Inertial Sensory Bias Compensation

Nargess Sadeghzadeh Nokhodberiz, Javad Poshtan

Department of Electrical Engineering, Iran University of Science and Technology, Zip: 1684613114, Tehran, Iran
Emails: nargess_sadeghzadeh, jposhtan@iust.ac.ir

Received: May 2014 Revised: September 2014 Accepted: Dec. 2014

ABSTRACT:
In this paper, error dynamic model of Strapdown Inertial Navigation System (SINS) is employed for error compensation of Strapdown algorithm. Perfect visual sensor data is fused with inertial sensors to produce deviation vectors as noisy measurement models. Due to the high dimensional and sparse error dynamic, the system is decomposed to cascaded subsystems because of the system structure. Then, distributed (cascaded) Kalman filters (KFs) and state feedback compensators are designed according to interactions of subsystems. This not only speeds up computations and avoids error propagation but also makes tuning, debugging, and the verifying of the algorithm from the perspective of implementation easier and more precise. The proposed architecture is appropriate to be implemented by multiple processors. The experimental results based on data from 3D MEMS IMU and camera system are provided to demonstrate efficiency of the proposed method.

KEYWORDS: Strapdown Inertial Navigation System (SINS), Inertial Measurement Unit (IMU), Kalman Filtering, Cascaded State Estimation

1. INTRODUCTION

Inertial navigation is a self-contained navigation technique in which measurements provided by accelerometers and gyroscopes are used to track the position and orientation of an object relative to a known starting point, orientation, and velocity [1]. The small units consisting of accelerometers and gyroscopes are referred to as IMUs [2]. The evolution of small silicon based accelerometers and gyroscopes (Micro Electro Mechanical Systems (MEMS)), has made the use of INSs more widespread. Compared to traditional technology, MEMS components are small, light, inexpensive, have low power consumption and short start-up times. Currently, their major disadvantage is the reduced performance in terms of accuracy and bias stability [3]. The noisy and erroneous MEMS components cause the standalone use of MEMS sensors in SINS to deliver high level positioning errors for the applications of several seconds duration [4]. To overcome this problem, inertial sensors are typically used in combination with aiding sources such as vision, ultra-wideband (UWB) and the global positioning system (GPS) according to the application. The aiding sensor is chosen depending on the application. GPSs and UWBs are normally fused with inertial sensors to navigate autonomous vehicles in outdoor and indoor applications, respectively. They are used to stabilize the platform and follow a predetermined path. The combination of inertial sensors and vision is very suitable for applications in robotics and virtual reality (VR) [3]. In this paper, the SINS errors are compensated using the fusion of vision and inertial sensors. Besides, Kalman Filters [5] are employed to estimate the SINS errors modeled by a linear state space model.

Due to the complexity of Strapdown algorithm as well as the limitations of current processors in serial execution, the updating rate is not fast enough to support on line estimation in high dimensional systems. In order to deal with this problem, parallel computations instead of serial ones have been proposed more recently [6], [7]. Accordingly, the computation speed increases as a result of simultaneous computations, the algorithms can be better tuned and the implemented program can be easier debugged. Similarly in this paper, the derived error dynamic model is decomposed to subsystems. Cascaded decomposition and estimation paradigm is proposed for the system. The idea behind cascaded decomposition is that many systems such as the SINS error model can be structurally represented as cascaded, observable subsystems, which are less complex than the original system. The distributed setting is well suited to a cooperative modular implementation where each module has the task of observing one of the

subsystems, possibly using different methods, and relying on its own measurements and the information gathered from[1].

This paper is organized as follows. Some basic concepts are presented in Section 2. INS error dynamic model is formulated and decomposed in Section 3. Cascaded error estimation and compensation approaches are proposed in Section 4. Experimental results based on data from 3D MEMS IMU and camera system and discussions are provided in Section 5 to demonstrate the efficiency of the proposed methods. Finally, a summary is contained in Section 6.

2. PRELIMINARIES

In this section, basic concepts about inertial navigation system, faults of inertial sensors and IMU and visual measurement models are presented.

2.1. Inertial Navigation System

IMUs typically contain three orthogonal rate-gyroscopes and three orthogonal accelerometers, measuring angular velocity and linear acceleration, respectively. A moving body is described using two coordinate systems. The first one is on the body and referred to as B-system. However, it is important to describe it on an earth fixed coordinate system, referred to as the W-system. Since the measurements from the IMU system are made in B coordinate system, they should be transferred to the W-system using some transformation procedures [8]. Figure 1 depicts the relationship between B and W coordinate systems.

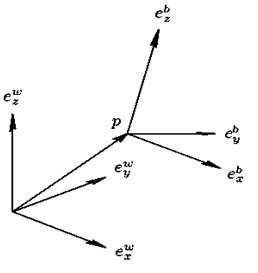

Fig. 1. The coordinate systems describing the moving body system. The coordinate system of $\left(e_x^b, e_y^b, e_z^b\right)$ is moving with the body, and the coordinate system $\left(e_x^w, e_y^w, e_z^w\right)$ is fixed [2].

By processing signals from these devices, it is possible to track the position and orientation of a device. All IMUs fall into two categories. The difference between them is the frame of reference in which the rate-gyroscopes and accelerometers operate. They are called "Stable Platform Systems" and "Strapdown Systems". In stable platform, sensors' platform is held in alignment with the global frame being kept fixed isolating from any external rotational motion. It is feasible to be mounted using gimbals. However, in "Strapdown systems" the inertial sensors are mounted rigidly onto the device, and therefore output quantities are measured in the body frame rather than the global frame. In this paper, we consider Strapdown systems. Orientation Tracking is kept by integrating the signals from the rate gyroscopes. To track position, the three accelerometer signals are resolved into global coordinates using the known orientation, as determined by the integration of the gyro signals. The global acceleration signals are then integrated as in the stable platform algorithm. This procedure is shown in Figure 2 [1].

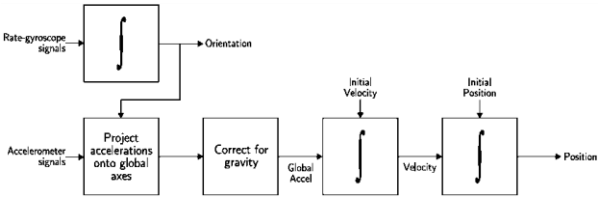

Fig. 2. Strapdown Inertial Navigation Algorithm [1]

2.2. Quaternions

In order to represent an attitude, we review attitude kinematics using quaternions. For attitude representation, quaternions have been most widely used. Quaternions are given by a four-dimensional vector defined as

$$\mathbf{q} = \begin{bmatrix} \cos(\delta/2) \\ \sin(\delta/2)\mathbf{n} \end{bmatrix} = \begin{bmatrix} q_0 \\ \bar{\mathbf{q}} \end{bmatrix}, \quad \bar{\mathbf{q}} = \begin{bmatrix} q_1 \\ q_2 \\ q_3 \end{bmatrix} \tag{1}$$

Where n is the unit Euler axis and δ is the rotation angle around n [9] and $\mathbf{q}$ is presented as a two-part vector. The first part is scalar part, q_0, and the second part is vector part, $\bar{\mathbf{q}}$. Rotation matrix can also be used to explain rotation. It is also exploited as a matrix multiplication to produce the rotated vector or for mapping a vector from one reference frame to another. Denote the rotation matrix as $\mathbf{R(q)}$. Then, this matrix maps a vector B_r in a reference frame $\mathbf{B}$ to a vector W_r in another frame $\mathbf{W}$, such that

$$w_r = \mathbf{R(q)}^B \mathbf{r} \tag{2}$$

Where

[1] Some parts of this work have been presented in 5th International Conference on Mechatronics (ICOM13), July 2013, Kuala Lumpur, Malaysia.

$$\mathbf{R}\left(\mathbf{q}=\begin{bmatrix}q_0\\q_1\\q_2\\q_3\end{bmatrix}\right)=\begin{bmatrix}q_0^2+q_1^2-q_2^2-q_3^2 & 2(q_1q_2+q_0q_3) & 2(q_1q_3-q_0q_2)\\ 2(q_1q_2-q_0q_3) & q_0^2-q_1^2+q_2^2-q_3^2 & 2(q_2q_3+q_0q_1)\\ 2(q_1q_3+q_0q_2) & 2(q_2q_3-q_0q_1) & q_0^2-q_1^2-q_2^2+q_3^2\end{bmatrix}$$

2.3. IMU Sensory Faults and INS Propagated Error

The measurements from real sensors are corrupted by errors. In general terms, the MEMS accelerometers, and gyroscopes measurements are disturbed with sensory biases and noises. Bias is a constant offset from the nominal sensor signal statistics. The angular velocity signals obtained from the gyroscopes are integrated by the standard INS attitude algorithm; therefore errors in the gyroscope signals propagate through the calculated orientation. In addition, errors which arise in the accelerometers propagate through the double integration. This is the obvious cause of drift in the tracked position. The important difference between errors arising from the accelerometers is that they are integrated twice in order to track position, whereas rate-gyro signals are only integrated once to track orientation [1], [10].

A general sensor output model used to describe the output of inertial sensors has the following form,

$$\mathbf{S}_m=\mathbf{S}_t+\mathbf{b}(t) \tag{3}$$

Where, $\mathbf{S}_m$ is the sensors' measured output. $\mathbf{S}_t$ is the true value of the quantity that the sensor is measuring and is corrupted by the general offset term of $\mathbf{b}(t)$. The offset term, $\mathbf{b}(t)$, has the following form,

$$\mathbf{b}(t)=\mathbf{b}_0+\mathbf{b}_n(t) \tag{4}$$

The term $\mathbf{b}_0$ represents constant offset or bias and the term $\mathbf{b}_n(t)$ represents the zero mean sampling noise with the covariance matrix of $\sigma_{b_n}^2\mathbf{I}_3$. By appropriate replacements the following measurement models are obtained,

$$\mathbf{y}_\omega(k)=\boldsymbol{\omega}(k)+\mathbf{b}_{0\omega}(k)+\mathbf{b}_\omega(k) \tag{5}$$

$$\mathbf{y}_a(k)=\mathbf{R}(\mathbf{q}).\left(\mathbf{a}\ (k)+\mathbf{b}_{0a}(k)+\mathbf{b}_a(k)\right) \tag{6}$$

Where, $\boldsymbol{\omega}$ is real angular velocity vector of the frame B relative to frame W, and $\mathbf{a}$ is acceleration vector in W coordinate system. $\mathbf{b}_{0\omega}$ and $\mathbf{b}_{0a}$ are the gyroscope and accelerometer bias vectors, respectively. $\mathbf{b}_\omega(k)\sim\mathcal{N}\left(\mathbf{0},\sigma_{\mathbf{b}_\omega}^2\mathbf{I}\right)$ and $\mathbf{b}_a(k)\sim\mathcal{N}\left(\mathbf{0},\sigma_{\mathbf{b}_a}^2\mathbf{I}\right)$ are the zero mean Gaussian sampling noises.

2.4. Visual Measurement Model

The visual sensor in this paper, comprises three cameras combined with three light sources (LEDs). They are employed for close range photogrammetry. Photogrammetry is the technique of measuring objects (2D or 3D) from photographic images and a set of colinearity explaining the relationship between the position/attitude matrix of the object and observations are used to determine the attitude of object [11]. The measurement model for quaternions and position are as follows,

$$\mathbf{y}_q(k)=\mathbf{q}(k)+\mathbf{v}_q(k) \tag{7}$$

$$\mathbf{y}_p(k)=\mathbf{p}(k)+\mathbf{v}_p(k) \tag{8}$$

Where $\mathbf{v}_p$, $\mathbf{v}_q$ are zero mean measurement noises with any known probability density function and covariance matrices of $\mathbf{R}_{v_p}$ and $\mathbf{R}_{v_q}$.

It is worth noting that, quaternion operations [9] has been approximated by normal operations in equation (7).

3. ERROR DYNAMIC MODEL FORMULATION AND DECOMPOSITION

In this section, inertial navigation system error dynamic model is derived and an appropriate tearing technique is proposed.

3.1. Error Dynamic Model Derivation

The INS error dynamic model is derived in this section. Since bias is a constant sensory fault, accelerometer and gyroscope bias dynamics are modeled as follows,

$$\mathbf{b}_{1a}(k+1)=\mathbf{b}_{1a}(k) \tag{9}$$

$$\mathbf{b}_{0\omega}(k+1)=\mathbf{b}_{0\omega}(k) \tag{10}$$

After propagation of accelerometer bias in SINS algorithm, the speed deviation, $\delta\mathbf{v}$, is resulted in the following dynamics,

$$\delta\mathbf{v}(k+1)=\delta\mathbf{v}(k)+T\mathbf{b}_{0a}(k) \tag{11}$$

Where, T is the sampling time. Similarly, the dynamics of position deviation, $\delta\mathbf{p}$, is obtained as follows,

$$\delta\mathbf{p}(k+1)=\delta\mathbf{p}(k)+T\delta\mathbf{v}(k) \tag{12}$$

Employing quaternion kinematics, the angular rate deviation is propagated through quaternion kinematics. The quaternions' kinematics is given by

$$\dot{\mathbf{q}}(t)=\frac{1}{2}\mathbf{S}'(\mathbf{q}).\boldsymbol{\omega} \tag{13}$$

Where

$$\mathbf{S}'(\mathbf{q}):=\begin{bmatrix}-q_1 & -q_2 & -q_3\\ q_0 & -q_3 & q_2\\ q_3 & q_0 & -q_1\\ -q_2 & q_1 & q_0\end{bmatrix}$$

Linearizing about zero attitude deviation of $\delta\mathbf{q}=\begin{bmatrix}1 & 0 & 0 & 0\end{bmatrix}^T$, and disregarding the quaternion

scalar element, $\delta q_0 = 1$, the following discretized error quaternion model is obtained,

$$\delta\bar{\mathbf{q}}(k+1) = \delta\bar{\mathbf{q}}(k) + \frac{T}{2}\mathbf{b}_{0\omega}(k) \tag{14}$$

Now, deviation state vectors of the translational and attitude subsystems are defined as follows,

$$\delta\mathbf{x}_{trans} := \begin{bmatrix} \delta\mathbf{p} \\ \delta\mathbf{v} \\ \mathbf{b}_{0a} \end{bmatrix},\ \delta\mathbf{x}_{att} := \begin{bmatrix} \delta\bar{\mathbf{q}} \\ \mathbf{b}_{0\omega} \end{bmatrix} \tag{15}$$

Accordingly, the error dynamics of the translational and attitude subsystems are reformulated as follows,

$$\delta\mathbf{x}_{trans}(k+1) = \mathbf{A}_{trans}\delta\mathbf{x}_{trans}(k) + \mathbf{B}_{trans}\boldsymbol{\eta}_{trans} \tag{16}$$

$$\delta\mathbf{x}_{att}(k+1) = \mathbf{A}_{att}\delta\mathbf{x}_{att}(k) + \mathbf{B}_{att}\boldsymbol{\eta}_{att} \tag{17}$$

Where

$$\boldsymbol{\eta}_{trans} \sim \mathcal{N}\left(\mathbf{0}, \sigma^2_{\boldsymbol{\eta}_{trans}}\mathbf{I}\right)\ ,\ \mathbf{B}_{trans} = \begin{bmatrix} T^2\mathbf{I} & T\mathbf{I} & \mathbf{I} \end{bmatrix}^T$$

$$\mathbf{A}_{trans} = \begin{bmatrix} \mathbf{I} & T\mathbf{I} & \mathbf{0} \\ \mathbf{0} & \mathbf{I} & T\mathbf{I} \\ \mathbf{0} & \mathbf{0} & \mathbf{I} \end{bmatrix}$$

And

$$\boldsymbol{\eta}_{att} \sim \mathcal{N}\left(\mathbf{0}, \sigma^2_{\boldsymbol{\eta}_{att}}\mathbf{I}\right)\ ,\ \mathbf{B}_{att} = \begin{bmatrix} T\mathbf{I} & \mathbf{I} \end{bmatrix}^T$$

$$\mathbf{A}_{att} = \begin{bmatrix} \mathbf{I} & 0.5T\mathbf{I} \\ \mathbf{0} & \mathbf{I} \end{bmatrix},$$

3.2. Sensor Fusion

The required measurement model for the error dynamic model is obtained via sensor fusion. To this end, camera measurements ($\mathbf{y}_p$ and $\mathbf{y}_q$) are assumed to be almost perfect (low noise level and fault free) and the propagated error through the Strapdown algorithm is obtained by simply subtracting the outputs of Strapdown algorithm ($\mathbf{p}_{IMU-Strap}$ and $\mathbf{q}_{IMU-Strap}$) and camera measurements, as follows,

$$\mathbf{y}_{\delta\mathbf{p}} = \mathbf{y}_p - \mathbf{p}_{IMU-Strap} \tag{18a}$$

$$\mathbf{y}_{\delta\mathbf{q}} = \mathbf{y}_q - \mathbf{q}_{IMU-Strap} \tag{18b}$$

3.3. System Decomposition and Measurement Model Extraction

The high dimensional (15^{th} dimension) IMU error dynamic system is considered as a large scale system following Jamshidi's definition of large scale systems [12]. It implies that a system is considered to be large scale if it can be partitioned or decoupled into a number of subsystems. Besides, the sparseness of the system matrix also causes computational complexity. To reduce the complexity, speed up the computations and provide an accurate debugging from the perspective of programming, it is proposed to decompose the system into observable subsystems as system structuring is a crucial step to deal with complexity.

Fundamental decomposition schemes are based either on functional decomposition or on structural decomposition. In functional approach of the decomposition a system is split in its functional, physical, or behavioral components. For example a system can be functionally split in sensors, controllers, and actuators and can be separated behaviorally to its basic dynamic behaviors such as linear or nonlinear subsystems. However, structural decomposition represents how the different parts of the system interact with each other leading to system graph representation [13], [14] and [15]. For the error system, described in previous parts, a structural cascaded decomposition of the system model is proposed. According to this structure, a system is decomposed into subsystems in a cascaded manner. Interactions only take place between neighboring levels through well-defined interfaces. In cascaded decomposition, the state of the first subsystem is considered as the input of the second subsystem and so on.

A necessary and sufficient condition for the existence of cascaded system decomposition is that the system and measurement matrices can be transformed into block lower-triangular forms [14]. Accordingly, it is necessary to generate more measurement models computationally and through computational differentiation of the measurement models of (18a) and (18b). Accordingly, the following measurement models are obtained,

$$\mathbf{y}_{trans}(k) = \begin{bmatrix} \mathbf{y}_{\delta\mathbf{p}}(k) \\ \mathbf{y}_{\delta\mathbf{v}}(k) \\ \mathbf{y}_{\mathbf{b}_a}(k) \end{bmatrix} = \mathbf{C}_{trans}\delta\mathbf{x}_{trans}(k) + \mathbf{v}_{trans}(k) \tag{19a}$$

$$\mathbf{y}_{att}(k) = \begin{bmatrix} \mathbf{y}_{\delta\mathbf{q}}(k) \\ \mathbf{y}_{\mathbf{b}_\omega}(k) \end{bmatrix} = \mathbf{C}_{att}\delta\mathbf{x}_{att}(k) + \mathbf{v}_{att}(k) \tag{19b}$$

Where

$$\mathbf{C}_{att} = \mathbf{I}_{9\times 9},\ \mathbf{C}_{trans} = \mathbf{I}_{6\times 6}$$

$$\mathbf{y}_{\mathbf{b}_\omega} := \mathbf{y}_\omega(k) - \boldsymbol{\omega}(k) = \mathbf{b}_{0\omega}(k) + \mathbf{b}_\omega(k)$$

$$\mathbf{y}_{\mathbf{b}_a} := \mathbf{y}_a(k) - \mathbf{a}\ (k) = \mathbf{b}_{0a}(k) + \mathbf{b}_a(k)$$

$$\mathbf{v}_{trans}(k) = \begin{bmatrix} \mathbf{v}_{\mathbf{p}}(k) \\ \mathbf{v}_{\mathbf{v}}(k) \\ \mathbf{b}_a(k) \end{bmatrix},\ \mathbf{v}_{att}(k) = \begin{bmatrix} \mathbf{v}_{\mathbf{q}}(k) \\ \mathbf{b}_\omega(k) \end{bmatrix}$$

It is worth noting that only the white noises are related to acceleration and angular velocity error subsystems

and other noises of $\mathbf{v_p}$, $\mathbf{v_v}$ and $\mathbf{v_q}$ are actually colored with time varying covariances of $\frac{\sigma_{\mathbf{b}_a}^2}{3}T^4k^3\mathbf{I}$, $\sigma_{\mathbf{b}_a}^2T^2k\mathbf{I}$ and $\sigma_{\mathbf{b}_\omega}^2T^2k\mathbf{I}$, respectively. However, if the sampling time is assumed very small (msec) and the sample of k is assumed to be finite, the following approximations of noise characteristics are obtained,

$\mathbf{v}_{att} \sim \mathcal{N}(\mathbf{0}, \mathbf{Q}_{att})$ and $\mathbf{v}_{trans} \sim \mathcal{N}(\mathbf{0}, \mathbf{Q}_{trans})$

$$\mathbf{Q}_{att} \approx \sigma_{\mathbf{b}_\omega}^2 \begin{bmatrix} T\mathbf{I} & \mathbf{0} \\ \mathbf{0} & \mathbf{I} \end{bmatrix} = \begin{bmatrix} \mathbf{Q}_{1att} & \mathbf{0} \\ \mathbf{0} & \mathbf{Q}_{2att} \end{bmatrix} \text{ and}$$

$$\mathbf{Q}_{trans} \approx \sigma_{\mathbf{b}_a}^2 \begin{bmatrix} T\mathbf{I} & \mathbf{0} & \mathbf{0} \\ \mathbf{0} & T\mathbf{I} & \mathbf{0} \\ \mathbf{0} & \mathbf{0} & \mathbf{I} \end{bmatrix} = \begin{bmatrix} \mathbf{Q}_{1trans} & \mathbf{0} & \mathbf{0} \\ \mathbf{0} & \mathbf{Q}_{2trans} & \mathbf{0} \\ \mathbf{0} & \mathbf{0} & \mathbf{Q}_{3trans} \end{bmatrix}$$

According to the proposed cascaded tearing paradigm, the system is partitioned to three behavioral cascaded subsystems for translational, as follows,

$$\mathbf{x}_{1trans} := \delta\mathbf{p};\ \ \mathbf{x}_{2trans} := \delta\mathbf{v};\ \ \mathbf{x}_{3trans} := \mathbf{b}_{0a} \tag{20}$$

Accelerometer bias subsystem:

$$\mathbf{x}_{3trans}(k+1) = \mathbf{A}_{33trans}\mathbf{x}_{3trans}(k) + \mathbf{B}_{3trans}\boldsymbol{\eta}_{3trans} \tag{21a}$$

$$\mathbf{y}_{3trans}(k) = \mathbf{C}_{3trans}\mathbf{x}_{3trans}(k) + \mathbf{v}_{\mathbf{p}}(k) \tag{21b}$$

Speed error subsystem:

$$\mathbf{x}_{2trans}(k+1) = \mathbf{A}_{22trans}\mathbf{x}_{1trans}(k) + \mathbf{A}_{23trans}.\mathbf{x}_{2trans}(k) + \mathbf{B}_{2trans}\boldsymbol{\eta}_{2trans} \tag{22a}$$

$$\mathbf{y}_{2trans}(k) = \mathbf{C}_{2trans}\mathbf{x}_{2trans}(k) + \mathbf{v}_{\mathbf{v}}(k) \tag{22b}$$

Position error subsystem:

$$\mathbf{x}_{1trans}(k+1) = \mathbf{A}_{11trans}\mathbf{x}_{1trans}(k) + \mathbf{A}_{12trans}.\mathbf{x}_{2trans}(k) + \mathbf{B}_{1trans}\boldsymbol{\eta}_{1trans} \tag{23a}$$

$$\mathbf{y}_{1trans}(k) = \mathbf{C}_{1trans}\mathbf{x}_{1trans}(k) + \mathbf{b}_a(k) \tag{23b}$$

Where

$$\mathbf{A}_{11trans} = \mathbf{A}_{22trans} = \mathbf{A}_{33trans} = \mathbf{C}_{1trans} = \mathbf{C}_{2trans} = \mathbf{C}_{3trans} = \mathbf{I}_{3\times3}$$
$$\mathbf{A}_{12trans} = \mathbf{A}_{23trans} = T\mathbf{I}_{3\times3},$$
$$\mathbf{B}_{1trans} = \mathbf{I}_{3\times3} \quad \mathbf{B}_{2trans} = T\mathbf{I}_{3\times3} \quad \mathbf{B}_{3trans} = T^2\mathbf{I}_{3\times3}$$

and two subsystems for attitude, as follows,

$$\mathbf{x}_{1att} := \delta\bar{\mathbf{q}};\ \ \mathbf{x}_{2att} := \mathbf{b}_{0\omega} \tag{24}$$

Gyroscope bias subsystem:

$$\mathbf{x}_{2att}(k+1) = \mathbf{A}_{22att}\mathbf{x}_{2att}(k) + \mathbf{B}_{2att}\boldsymbol{\eta}_{2att} \tag{25a}$$

$$\mathbf{y}_{2att}(k) = \mathbf{C}_{2att}\mathbf{x}_{1att}(k) + \mathbf{v}_{\mathbf{q}}(k) \tag{25b}$$

Angular rate error subsystem:

$$\mathbf{x}_{1att}(k+1) = \mathbf{A}_{11att}\mathbf{x}_{1att}(k) + \mathbf{A}_{12att}.\mathbf{x}_{2att}(k) + \mathbf{B}_{1att}\boldsymbol{\eta}_{1att} \tag{26a}$$

$$\mathbf{y}_{1att}(k) = \mathbf{C}_{1att}\mathbf{x}_{1att}(k) + \mathbf{b}_\omega(k) \tag{26b}$$

Where

$$\mathbf{A}_{11att} = \mathbf{A}_{22att} = \mathbf{C}_{1att} = \mathbf{C}_{2att} = \mathbf{I}_{3\times3}$$
$$\mathbf{A}_{12att} = T\mathbf{I}_{3\times3},\ \mathbf{B}_{1att} = \mathbf{I}_{3\times3}\ \ \mathbf{B}_{2att} = T\mathbf{I}_{3\times3}$$

4. DISTRIBUTED ERROR ESTIMATION AND COMPENSATION

In this section, firstly, separate observers are designed for each subsystem introduced in previous section (equations (20) to (26)). Then, an error compensation procedure is presented.

4.1. Cascaded Error Estimation

The proposed estimation architecture is depicted in Figure 3. Similar to centralized KF, cascaded KFs are designed by minimization of the trace of estimation error covariance. Accordingly, the following equations are obtained for position error subsystem to update Kalman error covariance and Kalman gain,

$$\mathbf{P}_{1trans}(k) = (\mathbf{I} - \mathbf{K}_{1trans}\mathbf{C}_{1trans})\mathbf{P}_{1trans}(k|k-1)(\mathbf{I} - \mathbf{K}_{1trans}\mathbf{C}_{1trans})^T + \mathbf{K}_{1trans}\mathbf{R}_{1trans}\mathbf{K}_{1trans}^T \tag{27a}$$

$$\mathbf{K}_{1trans}(k) = \mathbf{P}_{1trans}(k|k-1)\mathbf{C}_{1trans}^T\left(\mathbf{C}_{1trans}\mathbf{P}_{1trans}(k|k-1)\mathbf{C}_{1trans}^T + \mathbf{R}_{1trans}\right)^{-1} \tag{27b}$$

$$\mathbf{P}_{1trans}(k|k-1) = \mathbf{A}_{11trans}\mathbf{P}_{1trans}(k-1)\mathbf{A}_{11trans}^T + \mathbf{A}_{12trans}\mathbf{P}_{2trans}(k-1)\mathbf{A}_{12trans}^T + \mathbf{Q}_{1trans} \tag{27c}$$

Where it is assumed that the estimation error covariance matrix is block diagonal, that is,

$$\mathbf{P}_{trans} = \begin{bmatrix} \mathbf{P}_{1trans} & \mathbf{0} & \mathbf{0} \\ \mathbf{0} & \mathbf{P}_{2trans} & \mathbf{0} \\ \mathbf{0} & \mathbf{0} & \mathbf{P}_{3trans} \end{bmatrix} \tag{28}$$

However, this condition appears restrictive in practice and one rarely knows the true cross covariances and it is often assumed that the covariance matrix is diagonal [14].

Similarly, Kalman gains and error covariance matrices are calculated for the other subsystems.

4.2. Distributed Error Compensation

The bias of the Strapdown system is corrected by state regulators. The deviations can almost be corrected manipulating Strapdown algorithm using normal state

feedback controllers. Figure 4 depicts the schematic of cascaded error estimation and compensation for translational subsystems where, K_{acc}, K_{vel} and K_{pos} are state feedback gains related to acceleration bias, velocity and position errors, respectively.

5. EXPERIMENTAL RESULTS

In this section, experimental results based on data from 3D MEMS IMU and 3D camera system are analyzed and discussions are provided to investigate the efficiency of the proposed method. The structure of the camera, IMU and rigid body is depicted in Figure 5. The Crista IMU three-axis inertial sensor is exploited. It consists of MEMS gyroscopes and accelerometers mounted on orthogonal axes to provide 300 0/s rate and 10g acceleration [16]. High speed and high accuracy, K600 Krypton Camera, is used to precisely measure the position of static and dynamic targets in 3-D space. The real data gathered at a sampling rate of 1 KHz from IMU and Camera system interfaced with QNX Neutrino RTOS [17] in target-host architecture in 30 sec. They are then processed offline using MATLAB 2008 in mfile environment with sampling rate of 0.05 sec. The results have been presented in figures 6 to 8 for both compensated and non-compensated cases for translational subsystem. It can be easily seen that the biases and errors are compensated using the proposed approach and when they are not compensated, the speed and position deviations increase linearly and quadratically, respectively because of Strapdown integrations.

Other advantages of the proposed modular approach reside not only in easier debugging and more efficient computations but also it leads to less computational time compared with centralized approach. In order to obtain an estimation of each subsystem states in central architecture, it is necessary to wait for the whole algorithm to be performed. However, in the cascaded or any other modular architecture, the estimation of each subsystem is computed separately. So, less computational time is needed for each subsystem. For example, in one simulation in MATLAB mfile, estimation of bias acceleration takes 0.943 ms in the central approach; however, it takes 0.4 ms in the cascaded structure. Computation time is an important factor in most of engineering problems such as fault diagnosis, where it is so important to detect and isolate faults in time avoiding its propagation through the whole system. It is worth noting that this time has been computed when it is simulated in a single processor, however, using multi-processors leads to smaller computation time.

Despite the advantages, the linearization of nonlinear quaternion dynamic can be mentioned as the method drawback.

6. CONCLUSION

In this paper, a cascaded structure for error estimation and compensation of inertial navigation system was employed. Perfect visual sensor data was fused with inertial sensors to provide deviation vectors as noisy measurement models. High dimensional and sparse error dynamic was decomposed to cascaded subsystems and cascaded KFs and state feedback compensators were designed accordingly. The efficiency of the proposed method were evaluated from different aspects of computation time, estimation accuracy and error compensation using experimental results based on data from a 3D MEMS IMU and a 3D camera system.

7. ACKNOWLEDGMENT

We are grateful to Prof. Dr. Sc. Techn. Essam Badreddin, Dr. Achim Wagner and Dipl.-Inf. Eugen Nordheimer at Automation Laboratory, University of Heidelberg, Mannheim, Germany, whose outstanding efforts have made these experiments possible.

REFERENCES

[1] O. J. Woodman, "An Introduction to Inertial Navigation",. Computer Laboratory , University of Cambridge, . August 2007. Technical reports.

[2] D. Törnqvist, **"Statistical Fault Detection with Applications to IMU Disturbances"**, *Department of Electrical Engineering, Division of Automatic Control, Linköping university. Linköping* : Linköping University Electronic Press, 2006. PhD Dissertation.

[3] J. Hol, **"Sensor Fusion and Calibration of Inertial Sensors, Vision,Ultra-Wideband and GPS"**, *Department of Electrical Engineering*, Linköping : Linköping University Electronic Press, 2011. Phd Dissertation. 1368.

[4] D. Li, R. J. Landry, and P. Lavoie, **"Low-cost MEMS Sensor-based Attitude Determination System by Integration of Magnetometers and GPS: A Real-Data Test and Performance Evaluation"**, *IEEE/ION Position, Location and Navigation Symposium*, 2008, pp. 1190-1198.

[5] M. S. Grewal, **"Kalman Filtering: Theory and Practice using MATLAB"**, s.l. : *Wiley-Inter-Science Publication*, 2001. Vol. 1.

[6] Z. T. Sensors, T. J. Li, C. L. Wu, L. H. Lin, **"Field Programmable Gate Array Based Parallel Strapdown Algorithm Design for Strapdown Inertial Navigation Systems"**, Ma. 8, 2011, Vol. 11, pp. 7993-8017.

[7] M. Jew, A. El-Osery, S. Bruder, **"Implementation of an FPGA-based aided IMU on a low-cost autonomous outdoor robot"**, *IEEE/ION Position Location and Navigation Symposium (PLANS 2010)* Indian Wells, CA : s.n., May 2010., pp. 1043-1051.

[8] D. Törnqvist, **"Statistical Fault Detection with Applications to IMU Disturbances"**, Department of Electrical Engineering, Division of Automatic Control, *Linköping university. Linköping :*

Linköping University Electronic Press, 2006. PhD Dissertation.

[9] D. Törnqvist. **"Estimation and Detection with Applications to Navigation"**, Department of Electrical Engineering, Division of Automatic Control, *Linköping university. s.l. : Linköping University Electronic Press*, 2008. PhD Dissertation.

[10] E. Balaban, A. Saxena, P. Bansal, K. F. Goebel, and S. Curran, **"Modelling Detection and Disambiguation of Sensor Faults for Aerospace Applications"**, 12, *New York : IEEE Sensors Journal*, Vol. 9, 2009.

[11] S. G. Kim, J. L. Crassidis, Y. Cheng, A. M. Fosbury, and J. L. Junkins, **"Kalman Filtering for Relative Spacecraft Attitude and Position Estimation"**, *AIAA Guidance, Navigation & Control Conference and Exhibition*, Sanfrancisco, California : s.n., 2005.

[12] M. Jamshidi, **"Control of Large Scale Systems"**, *Control Systems, Robotics, and Automation*, Vol. XI, 2009.

[13] R. Ferrari, **"Distributed Fault Detection and Isolation of Large-scale Nonlinear Systems: an Adaptive Approximation Approach"**, *University of Trieste. Trieste Italy : ANNO ACCADEMICO*, 2008. PhD dissertation.

[14] Zs. Lendek, R. Babu˘ska, and B. De Schutter, **"Distributed Kalman filtering for cascaded systems"**, *Engineering Applications of Artificial Intelligence*, Vol. 21, 2008, pp. 457–469.

[15] M. Farina, G. Ferrari Trecate, **"Decentralized and Distributed Control: Models of Large Scale Systems"**, *Supelec, France : Graduate School on Control*, 2013.

[16] W. S. Flenniken, J. H. Wall, and D. M. Bevly, **"Characterization of Various IMU Error Sources and the Effect on Navigation Performance"**, *Proceedings of ION GNSS 18th International Technical Meeting of the Satellite Division*, 2005.

[17] R. Krten, **"QNX Neutrino RTOS: Getting Started with QNX Neutrino: A Guide for Realtime Programmers"**, *s.l. : QNX Software Systems International Corporation*,, 2009.

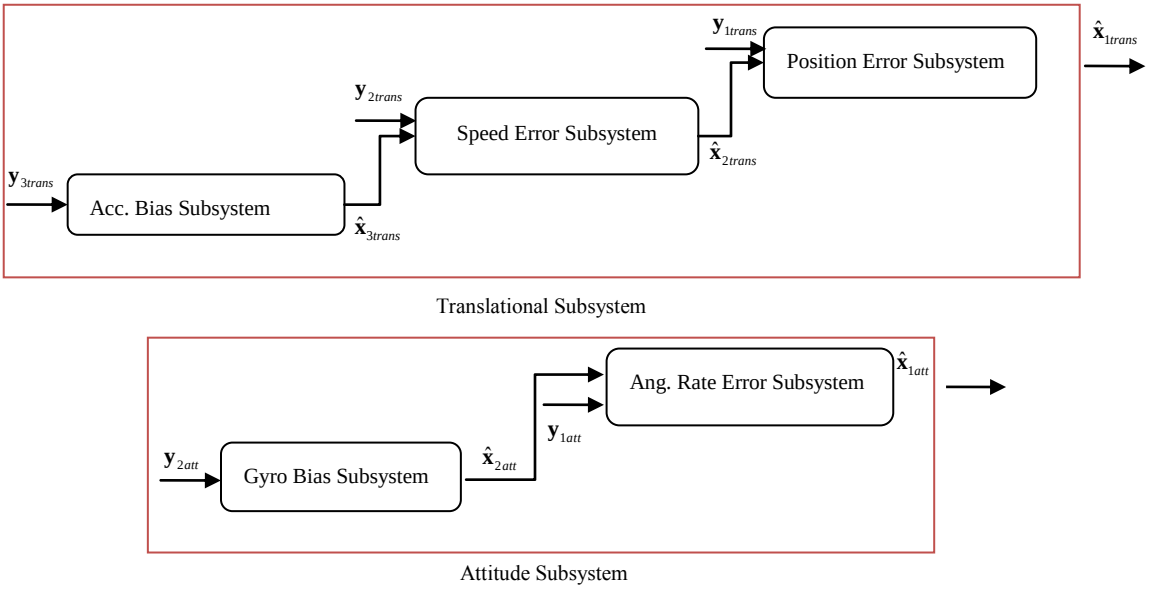

Fig. 3. Multi-Level Cascaded Estimator

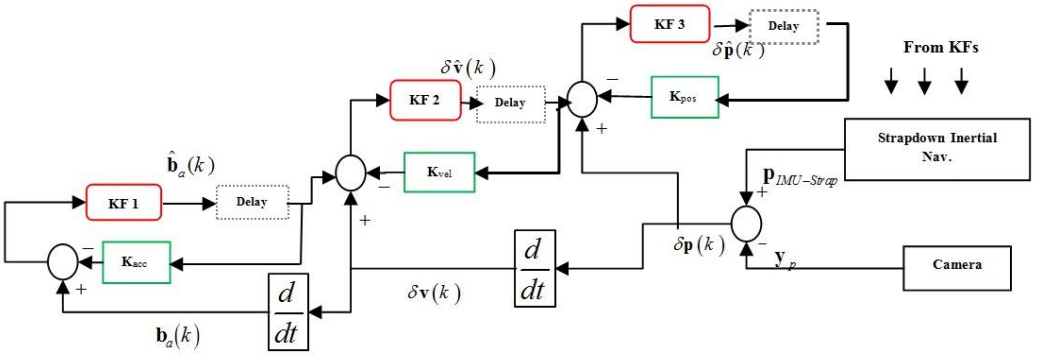

Fig. 4. Schematic of cascaded error estimation and compensation for translational subsystem (Kacc, K_{vel} and K_{pos} are state feedback gains related to acceleration bias, velocity and position errors, respectively)

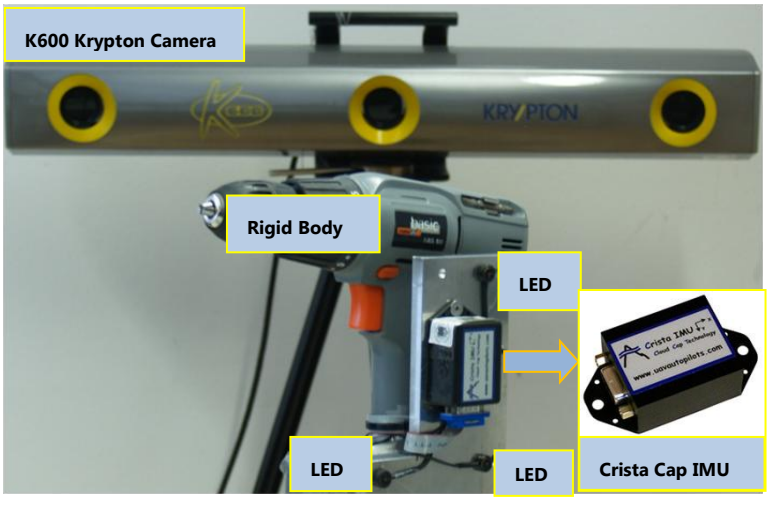

Fig. 5. Camera system, IMU and rigid body

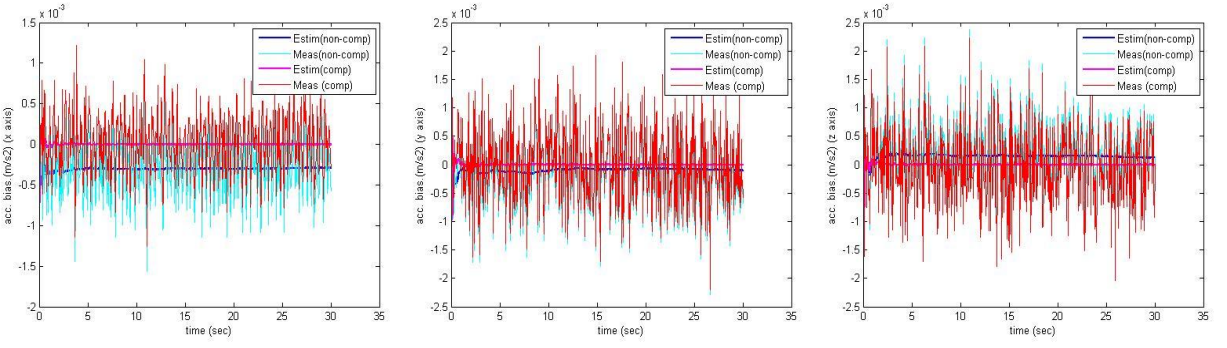

(a) x axis **(b) y axis** **(c) z axis**

Fig. 6. Accelerometer Bias: Estimations and measurements for both compensated and non-compensated cases

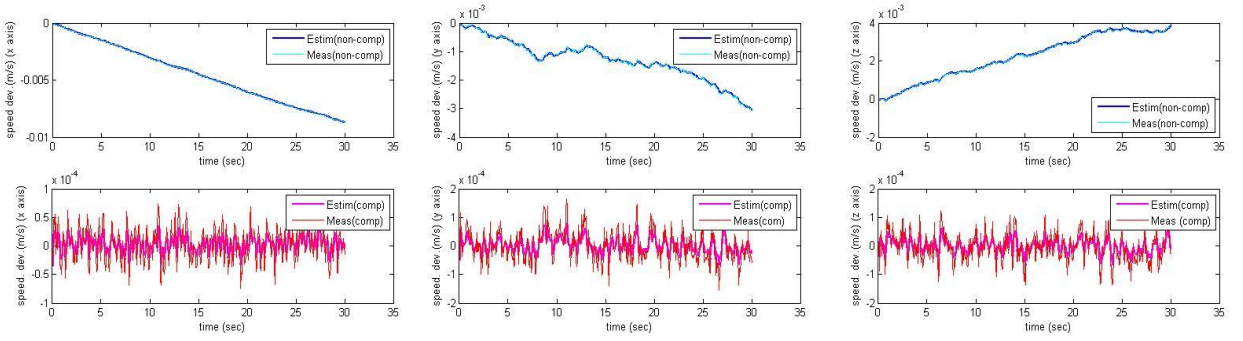

(a) x axis **(b) y axis** **(c) z axis**

Fig. 7. Speed Deviation: Estimations and measurements for both compensated and non-compensated cases

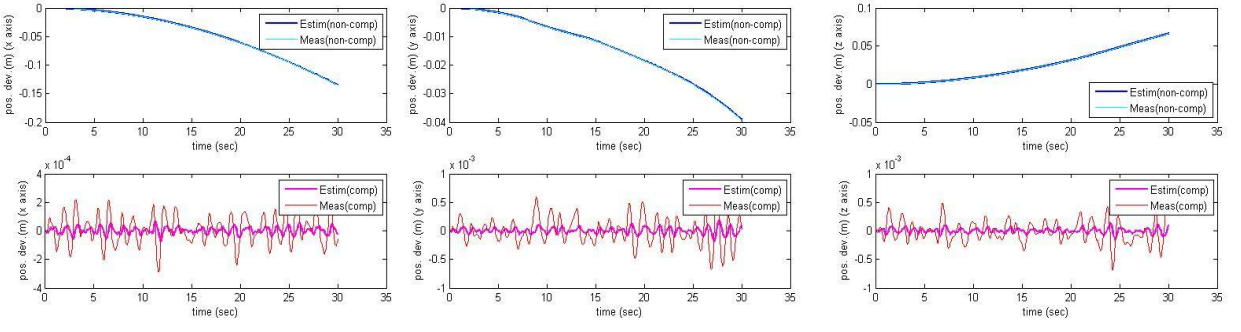

(a) x axis **(b) y axis** **(c) z axis**

Fig. 8. Position Deviation: Estimations and measurements for both compensated and non-compensated cases